The LISA Pathfinder Mission

The LISA Pathfinder Mission

M Armano[a], H Audley[b], G Auger[c], J Baird[n], P Binetruy[c], M Born[b], D Bortoluzzi[d], N Brandt[e], A Bursi[t], M Caleno[f], A Cavalleri[g], A Cesarini[g], M Cruise[h], K Danzmann[b], I Diepholz[b], R Dolesi[g], N Dunbar[i], L Ferraioli[j], V Ferroni[g], E Fitzsimons[e], M Freschi[a], J Gallegos[a], C García Marirrodriga[f], R Gerndt[e], LI Gesa[k], F Gibert[k], D Giardini[j], R Giusteri[g], C Grimani[l], I Harrison[m], G Heinzel[b], M Hewitson[b], D Hollington[n], M Hueller[g], J Huesler[f], H Inchauspé[c], O Jennrich[f], P Jetzer[o], B Johlander[f], N Karnesis[k], B Kaune[b], N Korsakova[b], C Killow[p], I Lloro[k], R Maarschalkerweerd[m], S Madden[f], D Mance[j], V Martín[k], F Martin-Porqueras[a], I Mateos[k], P McNamara[f], J Mendes[m], L Mendes[a], A Moroni[t], M Nofrarias[k], S Paczkowski[b], M Perreur-Lloyd[p], A Petiteau[c], P Pivato[g], E Plagnol[c], P Prat[c], U Ragnit[f], J Ramos-Castro[qr], J Reiche[b], J A Romera Perez[f], D Robertson[p], H Rozemeijer[f], G Russano[g], P Sarra[t], A Schleicher[e], J Slutsky[s], C F Sopuerta[k], T Sumner[n], D Texier[a], J Thorpe[s], C Trenkel[i], H B Tu[g], D Vetrugno[g], S Vitale[g], G Wanner[b], H Ward[p], S Waschke[n], P Wass[n], D Wealthy[i], S Wen[g], W Weber[g], A Wittchen[b], C Zanoni[d], T Ziegler[e], P Zweifel[j]

[a] European Space Astronomy Centre, European Space Agency, Villanueva de la Cañada, 28692 Madrid, Spain
[b] Albert-Einstein-Institut, Max-Planck-Institut für Gravitationsphysik und Universität Hannover, 30167 Hannover, Germany
[c] APC UMR7164, Université Paris Diderot, Paris, France
[d] Department of Industrial Engineering, University of Trento, via Sommarive 9, 38123 Trento, and Trento Institute for Fundamental Physics and Application / INFN
[e] Airbus Defence and Space, Claude-Dornier-Strasse, 88090 Immenstaad, Germany
[f] European Space Technology Centre, European Space Agency, Keplerlaan 1, 2200 AG Noordwijk, The Netherlands
[g] Dipartimento di Fisica, Università di Trento and Trento Institute for Fundamental Physics and Application / INFN, 38123 Povo, Trento, Italy
[h] Department of Physics and Astronomy, University of Birmingham, Birmingham, UK
[i] Airbus Defence and Space, Gunnels Wood Road, Stevenage, Hertfordshire, SG1 2AS, UK
[j] Institut für Geophysik, ETH Zürich, Sonneggstrasse 5, CH-8092, Zürich, Switzerland
[k] Institut de Ciències de l'Espai (CSIC-IEEC), Campus UAB, Facultat de Ciències, 08193 Bellaterra, Spain
[l] Istituto di Fisica, Università degli Studi di Urbino/ INFN Urbino (PU), Italy
[m] European Space Operations Centre, European Space Agency, 64293 Darmstadt, Germany
[n] The Blackett Laboratory, Imperial College London, UK
[o] Physik Institut, Universität Zürich, Winterthurerstrasse 190, CH-8057 Zürich, Switzerland
[p] SUPA, Institute for Gravitational Research, School of Physics and Astronomy, University of Glasgow, Glasgow, G12 8QQ, UK
[q] Department d'Enginyeria Electrònica, Universitat Politècnica de Catalunya, 08034 Barcelona, Spain

[r] Institut d'Estudis Espacials de Catalunya (IEEC), C/ Gran Capità 2-4, 08034 Barcelona, Spain
[s] NASA Goddard Space Flight Center, 8800 Greenbelt Road, Greenbelt, MD 20771, USA
[t] CGS S.p.A, Compagnia Generale per lo Spazio, Via Gallarate, 150 - 20151 Milano, Italy

E-mail: paul.mcnamara@esa.int

Abstract. LISA Pathfinder (LPF), the second of the European Space Agency's Small Missions for Advanced Research in Technology (SMART), is a dedicated technology validation mission for future spaceborne gravitational wave detectors, such as the proposed eLISA mission. LISA Pathfinder, and its scientific payload - the LISA Technology Package - will test, in flight, the critical technologies required for low frequency gravitational wave detection: it will put two test masses in a near-perfect gravitational free-fall and control and measure their motion with unprecedented accuracy. This is achieved through technology comprising inertial sensors, high precision laser metrology, drag-free control and an ultra-precise micro-Newton propulsion system. LISA Pathfinder is due to be launched in mid-2015, with first results on the performance of the system being available 6 months thereafter.

The paper introduces the LISA Pathfinder mission, followed by an explanation of the physical principles of measurement concept and associated hardware. We then provide a detailed discussion of the LISA Technology Package, including both the inertial sensor and interferometric readout. As we approach the launch of the LISA Pathfinder, the focus of the development is shifting towards the science operations and data analysis - this is described in the final section of the paper

1. Introduction

LISA Pathfinder, the second of the European Space Agency's Small Missions for Advanced Research in Technology (SMART), is a technology validation mission for future low frequency, spaceborne, laser interferometric gravitational wave detectors. When adopted by the European Space Agency (ESA) in 2004, LISA Pathfinder was a precursor for the joint ESA/NASA mission, LISA (Laser Interferometer Space Antenna) [1]. However, due to budget constraints at NASA, the partnership was dissolved in 2011, and LISA was reformulated as an ESA-only mission called the New Gravitational-wave Observatory (NGO) [2]. NGO was proposed to ESA as the first Large-class mission (L1) in its Cosmic Visions (CV) programme. However, it was not selected.

The NGO concept was further refined and renamed eLISA (evolved-LISA). This concept was included as the strawman mission design included in the science white-paper, *The Gravitational Universe* [3], submitted to the ESA call for science themes for the 2nd and 3rd Large-class missions in the CV programme. After review, *The Gravitational Universe* was selected as the science theme for the 3rd Large-class mission.

LISA, and variants of the LISA mission concept, have continually been ranked as one of the most scientifically important missions under study [4]. However the very concept of low frequency gravitational wave detection, *i.e.* that a particle falling under the influence of gravity alone can be isolated to follow a geodesic in spacetime, has never been demonstrated to the required precision. This is the most basic assumption of Einstein's General Relativity: LISA Pathfinder was selected by the European Space Agency to experimentally demonstrate this hypothesis with unprecedented accuracy.

LISA Pathfinder essentially mimics one arm of the eLISA constellation by shrinking the 1 million kilometre armlength down to a few tens of centimetres, giving up the sensitivity to gravitational waves, but keeping the measurement technology. The scientific objective of the LISA Pathfinder mission consists then of the first in-flight test of low frequency gravitational wave detection metrology.

LISA Pathfinder was first proposed in 1998 as ELITE (European LIsa Technology

Experiment) [5]. This mission consisted of a single spacecraft in geostationary orbit with a differential acceleration goal of $10^{-14}\,\mathrm{ms}^{-2}/\sqrt{\mathrm{Hz}}$ over a frequency range of 1-100 mHz. This original proposal was refined and proposed to ESA in 2000 in response to the SMART-2 announcement of opportunity. At the time, the proposal called for a joint LISA and Darwin pathfinder mission, consisting of two free-flying spacecraft, with three payloads (LISA Technology Package, Darwin Technology Package, and a NASA provided LISA Technology Package). The goal of the mission was to demonstrate drag-free control (for LISA) and formation flying (for Darwin). The mission was approved by the Science Programme Committee (SPC) in November 2000. After an initial industrial study, the mission was descoped to a single spacecraft (the Darwin Pathfinder was cancelled) and renamed LISA Pathfinder (LPF). At the time, LPF carried two payloads, the European built LISA Technology Package (LTP), and the NASA provided Disturbance Reduction System (DRS). Both payloads consisted of two inertial sensors, a laser metrology system, micro-Newton thrusters and drag free control software. However, the DRS was descoped and now consists of micro-Newton thrusters and a dedicated processor running the drag-free and attitude control software, and will rely on the LTP for its inertial sensing capability.

LISA Pathfinder is due to be launched in 2015 on-board a dedicated small launch vehicle. The launcher selected is the European VEGA launcher, which will launch LPF from the European spaceport of Kourou (French Guyana) into a parking orbit with perigee at 200 km, apogee at ≈ 1600 km, and an inclination to the equator of 5.3^{o}. After a series of apogee raising manoeuvres using an expendable propulsion module, LISA Pathfinder will enter a transfer orbit towards the first Sun-Earth Lagrange point (L1). After separation from the propulsion module, the LPF spacecraft will be stabilised using the micro-Newton thrusters, entering a 500,000 km by 800,000 km Lissajous orbit around L1.

Following the initial on-orbit check-out and instrument calibration, the in-flight demonstration of the LISA technology will then take place. The nominal lifetime of the science operations is 180 days; this includes the LTP and DRS operations.

2. The physics of LISA Pathfinder

eLISA will detect gravitational waves in the tidal acceleration they cause between distant free-falling test particles. This relative acceleration is observable in the variation of the Doppler frequency shift detected between a light beam received from the distant emitting test particle (e) and a local light beam generated with an equivalent laser at the receiver (r). The time derivative of this interference "Doppler beat note" can be expressed, for an optimal projection of gravitational wave strain h onto the axis defined by the test particles separation L,

$$\frac{\dot{\nu_r} - \dot{\nu_e}}{\nu} = \frac{1}{2}\left[\dot{h}\left(t\right) - \dot{h}\left(t - \frac{L}{c}\right)\right] + \frac{1}{c}\left[a_r\left(t\right) - a_e\left(t - \frac{L}{c}\right)\right] \ , \tag{1}$$

This highlights the competition of the gravitational wave signal with the difference in the acceleration between the two particles – or test masses, TM – due to any stray forces, measured relative to their locally free-falling reference frames at the time of emission and detection, $\Delta a \equiv \left[a_r\left(t\right) - a_e\left(t - \frac{L}{c}\right)\right]$, projected onto the axis separating the TM [6, 7]. This simple picture omits two complications relevant to eLISA: the Doppler shifts from laser frequency noise, handled by using two interferometry arms and time delay interferometry (TDI), and the composite nature of the TM-TM measurement, with a Doppler measurement between distant spacecraft (SC-SC) summed with two local measurements of relative TM-SC acceleration. At low frequencies, the eLISA noise budget is dominated by a relative stray TM acceleration Δa with spectral density $\sqrt{2} \times\ 3 \times 10^{-15}\ \mathrm{m/s^2/Hz^{1/2}}$.

LISA Pathfinder will demonstrate the possibility to perform a relative acceleration measurement between two TM in the same SC. The short, 38 cm, baseline, reduces the GW

strain term related to the change in $\dot{h}$ to an unresolvable level. However, it will measure the stray differential accleration noise from stray forces acting on two eLISA TM inside their respective gravitational reference sensors (GRS) – Δa between two nominally free-falling test particles – and demonstrate a local interferometric measurement of TM acceleration, at levels that can guarantee most of the eLISA science return.

The most sensitive differential acceleration measurements to date in the mHz frequency band come from the geodesy mission GOCE, of order 10^{-10} m/s^2/Hz$^{1/2}$ at mHz frequencies[8]. The LPF measurement configuration is essentially that of a gravity gradiometer, measuring one component – $\frac{\partial g_x}{\partial x}$ – of the 3 × 3 tensor measured by GOCE and, like GOCE, features rectangular parallelepiped TM of several cm dimensions inside conducting housings that provide capacitive position sensing and electrostatic force actuation. However, because of the big proposed leap forward in the differential acceleration measurement precision, to a specification of 3×10^{-14} m/s^2/Hz$^{1/2}$ at 1 mHz, LPF represents a truly new class of measurement. This improvement is made possible first by a change in location, from low earth orbit (LEO) to L1. This reduces the drag forces acting on the satellite, but also, more fundamentally, drastically reduces the gravity difference felt by the two TM, from the μm/s^2 level caused by Terrestrial gravity gradients in LEO to order nm/s^2, limited by the imperfect mass balancing of the LPF spacecraft itself, thus reducing the force noise introduced by actively compensating a large differential acceleration between the TM that limits a geodesy gradiometer. The residual difference in local g remains an important limitation for LPF and will be addressed shortly. To take advantage of this reduction in the required forcing, LPF and eLISA must correspondingly reduce other sources of stray forces, arising in large part in the interaction between the TM and the surrounding conducting shield that doubles as an electrostatic sensor and actuator, referred to collectively as the gravitational reference sensor (GRS). Compared to the hardware used in GOCE and other space accelerometry missions to date, the LPF GRS, presented in detail in Sec. 3.1, features much larger gaps between the TM and surrounding electrostatic sensor, removal of the conducting wire used to discharge the TM, and an overall mechanical and electronic design aimed at minimizing the force noise on the TM. The price of this design is the need for a UV TM discharge system, and, due to the large gaps, increased difficulty in caging the TM during launch vibration and a reduced capacitive position sensitivity, which requires the use of an interferometric readout of the TM position.

The central experiment of LISA Pathfinder is that of measuring the noise in the relative stray TM acceleration, the differential stray force per unit mass or, equivalently, the "open loop" differential acceleration that they would experience in the absence of any known or calibrated control or elastic coupling forces [9]. Considering the control of the actuation force on the SC along the critical x axis, in the main science mode, the thruster system uses a stiff, roughly 1 Hz bandwidth, controller to keep the SC centered on TM1 according to the o_1 readout of the TM1 displacement relative to the optical bench, $(x_1 - x_{SC})$ (Figure 1). An electrostatic control force, F_{ES}, is applied to the second TM, using a slow, roughly 1 mHz bandwidth, to maintain a fixed displacement of the two TM $(x_2 - x_1)$, according to the relative displacement interferometer readout o_{12} (Figure 1). The equations of motion for this system along the measurement x axis simplify to

$$\begin{aligned} \ddot{x}_1 &= a_1 - \omega_1^2 (x_1 - x_{SC}) \\ \ddot{x}_2 &= a_2 - \omega_2^2 (x_2 - x_{SC}) + \frac{F_{ES}}{m} \end{aligned} \tag{2}$$

where ω_1^2 and ω_2^2 represent springlike coupling or "stiffness" to the satellite motion, and a_1 and a_2 are the stray forces per unit mass acting on the two TM. Combining these two equations and

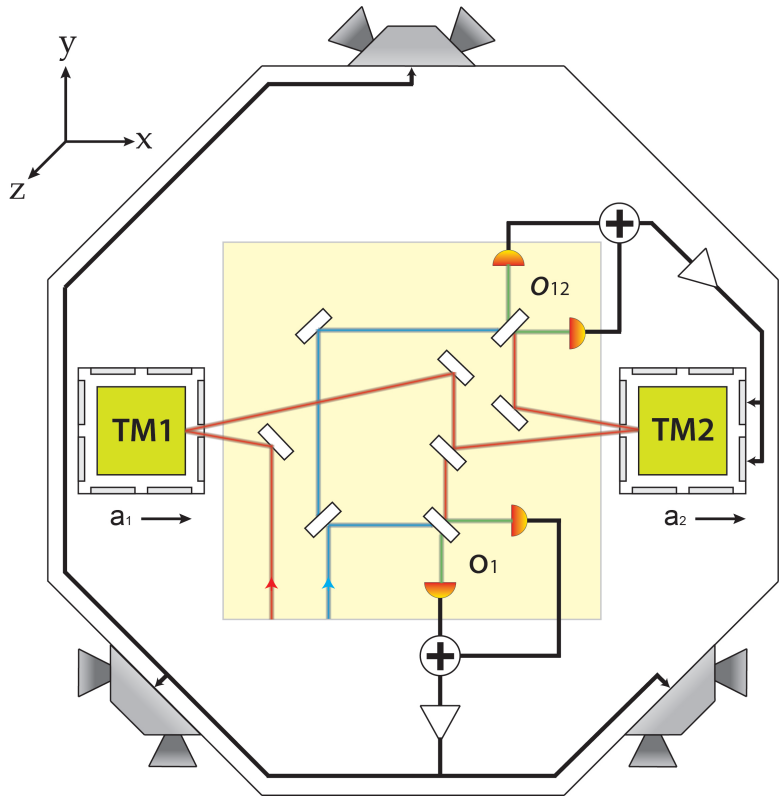

Figure 1. Cartoon of the LPF measurement configuration, showing the two TM inside their respective GRS housings, with an outline of the optical metrology for measuring the relative acceleration between the two TM (o_{12}) and that of TM1 relative to the spacecraft (o_1).

considering interferometric readout o_1 and o_{12}, allows generating $\Delta\hat{a}$, a time domain estimator of the differential stray force per unit mass,

$$\begin{aligned} \Delta\hat{a} &\equiv \ddot{o}_{12} - \frac{F_{ES}}{m} + \left(\omega_2^2 - \omega_1^2\right) o_1 + \omega_2^2 o_{12} \\ &= \Delta a + \ddot{n}_{12} + \left(\omega_2^2 - \omega_1^2\right) n_1 + \omega_2^2 n_{12} \end{aligned} \tag{3}$$

Thus $\Delta\hat{a}$ is an estimator of the desired differential stray acceleration, $\Delta a \equiv (a_2 - a_1)$. This is contaminated by noise in the interferometric displacement measurements, n_1 and n_{12}, directly in the differential acceleration $\ddot{n}_{12}$ but also, less significantly, in the calculation of the two stiffness coupling terms. This differential measurement of $\Delta\hat{a}$ also includes noise in the applied actuation force F_{ES}, which, as will be discussed later, is an important limiting factor in LPF but not in eLISA.

We note that the satellite coupling contributions are essentially subtracted off, along with the applied electrostatic forces, such that it is not the noisy satellite motion, but rather the *imprecision* in its measurement, that contributes noise through this elastic coupling. This requires that the parasitic stiffness ω_1, ω_2, and the scale factor for the commanded electrostatic actuators responsible for F_{ES}, be calibrated in a dedicated "system identification" experiment, in which large motion signals in both o_1 and o_{12} as well as large applied forces F_{ES} are excited, by applying modulated "guidance signals" that coherently move the drag-free and electrostatic

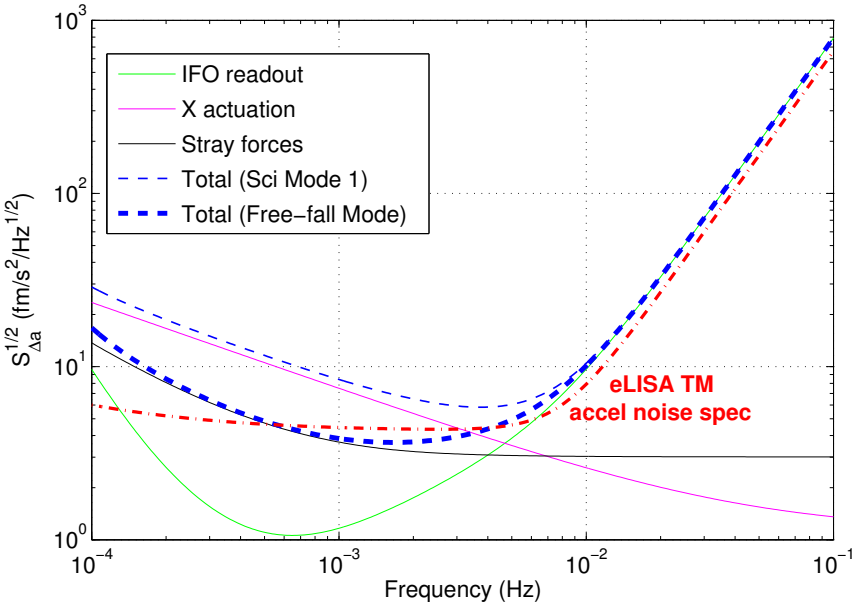

Figure 2. Current best estimates for the LPF differential acceleration noise measurement, in blue, with and without x axis force actuation, compared against the eLISA TM acceleration noise requirements in red (based mainly on the analysis in Ref.[10]).

controller setpoints. This measurement, and the data analysis strategy, will be discussed in Sec. 4.

Analysis of this main acceleration noise measurement will thus focus on an accurate estimation of the noise spectral density in $\Delta\hat{a}\,(t)$, with noise contributed by stray forces and interferometry noise. Our current best estimate of this stray acceleration noise measured in this configuration (known as "SCI Mode 1"), based on extensive ground testing with flight hardware and flight hardware prototypes in both torsion pendulum small force measurements and optical metrology tests, is shown in Fig. 2. The leading sources of force noise and interferometer measurement noise are discussed in Secs. 3.1 and 3.2.

As seen in the figure, the total low frequency acceleration noise in SCI Mode 1 is predicted to be dominated by the noise in the actuation along the x axis, which is needed to compensate the static spacecraft self-gravity imbalance between the two TM. Our estimate of this noise term is based on the target DC self-gravity imbalance limit of 0.65 nm/s^2, limited by modelling and integration precision of the spacecraft and payload mass, and an overall electrostatic actuator force stability, measured with the flight GRS FEE electronics to be slightly more than 10 ppm/Hz$^{1/2}$ at 1 mHz. Importantly, this force noise source is not present in eLISA, where two interferometry arms joining at a vertex ensure that the satellite control does not require TM forcing along the sensitive measurement axes: while LPF has two TM along a single sensitive axis in a single SC, requiring that one TM must be forced to follow the other, eLISA employs only a single TM per sensitive axis per spacecraft, and only spacecraft forcing is needed on these interferometry axes.

In order to measure the residual acceleration noise in the absence of this actuation noise which will not be present in eLISA, the LPF team is working on a "free-fall" mode experiment, in which the second TM is left free for periods up to several hundred seconds, in free-falling arcs of nearly parabolic motion – in nearly uniform sub-nano-g field relative to the inertial reference of TM1 – terminated by brief impulsive forces in order to limit the TM displacement and to compensate

the differential gravity imbalance *on average*. This leaves a gapped-data series of actuation-free acceleration noise to analyze [11]. As shown in Fig. 2, successful implementation of this free-fall mode would allow a significant improvement in the overall acceleration noise sensitivity at low frequencies, to the level of the eLISA TM acceleration noise requirement around 1 mHz. Testing the measurement sequence and analysis algorithms for this gapped and high-dynamic range data series in order to accurately estimate the underlying low-frequency acceleration noise is an important part of the ground preparation for LPF as we approach launch.

Performing a differential acceleration measurement approaching the eLISA requirements is one side of the LPF charter; creating a physical model that quantitatively describes the residual noise in this measurement, to apply to eLISA and other future ambitious experimental gravitational measurements, is the other. As such, the challenge in preparing for the LPF mission is that of defining a measurement program that, in additional to the main acceleration noise measurements, allows dedicated measurements to isolate, measure, and, in many cases, mitigate specific sources of both force noise and interferometry measurement noise. With the ability to both measure and controlledly modify the thermal, electrostatic, magnetic, and radiation environments seen by the TM and surrounding apparatus[12], as well as modify the dynamical control schemes and operating points, LPF will thus represent an orbiting laboratory for realizing high precision references of geodesic motion for fundamental physics experiments in space.

3. The LISA Technology Package

Unlike traditional observatory or planetary missions, the payload in LISA Pathfinder cannot be considered as a discrete piece of hardware carried by the spacecraft. Instead, during science operations, the payload and the spacecraft act as a single unit: the attitude control of the spacecraft is driven by the payload. LISA Pathfinder will carry two payloads; the LISA Technology Package (LTP), and the Disturbance Reduction System (DRS). The LISA Technology Package is provided by a consortium of European national space agencies (France, Germany, Italy, Spain, Switzerland, The Netherlands, and the United Kingdom) and ESA, while the DRS is provided by NASA. Only the LTP will be described here.

Figure 3 shows an artists impression of the LTP. The LTP consists of two major subsystems; the Inertial Sensor Subsystem, and the Optical Metrology Subsystem. Both subsystems are described in further detail in the following sections.

3.1. The Inertial Sensor Subsystem

Each of the two test masses is hosted in what is referred to as the 'Inertial Sensor Subsystem' (ISS), whose integration has been completed and is currently undergoing the final stages of testing prior to being integrated with the optical bench.

A schematic section of the ISS is shown in Fig. 4 and includes a dedicated vacuum chamber, a capacitive sensor electrode housing for TM actuation and position measurement, a caging system to secure the test mass during launch and to release it in flight, the UV vacuum fibre feedthrough for test mass charge management and the diagnostic items.

The test mass with the surrounding capacitive sensor constitute the Gravitational Reference Sensor (GRS), considered a key element for achieving the demanding test mass free-fall purity required by space-based gravitational wave detectors. The GRS for LISA Pathfinder has been designed to be suitable for use on board LISA-like missions [13] [14], with the overall force noise performance relaxed only to accommodate the x-axis actuation that is needed for LPF and for corresponding relaxations in the spacecraft electromagnetic and thermal environment.

With the electrode housing being the closest part to the test mass, it is potentially the most relevant disturbance source: careful design, implementation and performance verification strategy have been critical in achieving what was considered a very challenging goal.

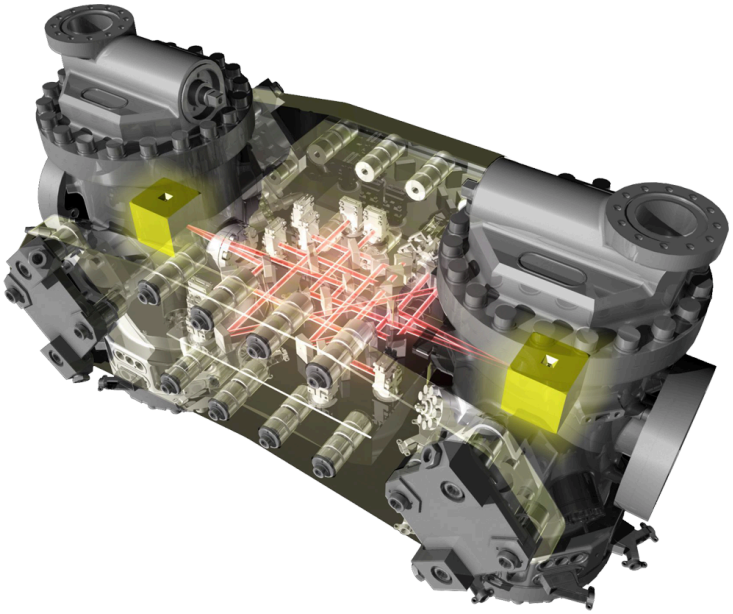

Figure 3. Artists impression of the LISA Technology Package (LTP). Credit: ESA

The electrode configuration design was driven by the need to have large gaps that reduce modelled and unmodelled surface forces, particularly from stray electrostatic potential fluctuations and Brownian motion from residual gas impacts, and by the aim of having comparable performance for all degrees of freedom in order to suppress possible cross-talk effects.

The configuration that has been chosen (see Fig. 5) is a rather symmetric, gap-sensing electrode design.

The main features include gaps of approximately 4 mm between the electrode housing and test mass, and injection electrodes on two axes instead of one to reduce off-axis stiffness. The choice of the test mass size was also important: in addition to the decrease in acceleration per given force with the total mass, increasing the TM size allows the surface area to achieve the 1.8 nm/Hz$^{1/2}$ displacement sensitivity needed for SC control on the yz axes, while limiting the electrostatic stiffness associated with the needed AC sensing bias to a negligible contribution.

The implementation of the electrode housing has been particularly challenging because of the numerous acceleration noise contributions related to employed materials, construction techniques, surface finishing and geometrical tolerances.

We mention here briefly just the effects that represented the main drivers. Temperature gradient fluctuations across the electrode housing cause a fluctuation of the stray acceleration due to the radiometric, radiation pressure and asymmetric outgassing effects. To limit these disturbances, it is important to use material with high thermal conductance and low outgassing rate. In addition, the level of outgassing rate sets the base pressure of the residual gas around the test mass that give rise to Brownian noise, one of the potential main entries in the acceleration noise budget around 1 mHz. A proper choice of material is not the only precaution to be taken in order to control the outgassing: finishing and preparation of the surfaces, their handling during the entire process of integration, and avoiding constructive solutions that may give rise to subtle virtual leaks are all aspects to be monitored very carefully.

In order to reduce the effect of stray voltages due to inhomogeneous contact potential, all TM and facing electrode housing surfaces should be coated with the same conductive material and unavoidable non-coated dielectric paths around the electrodes should be minimized and electrostatically shielded. The control of the GRS internal surface properties has been considered

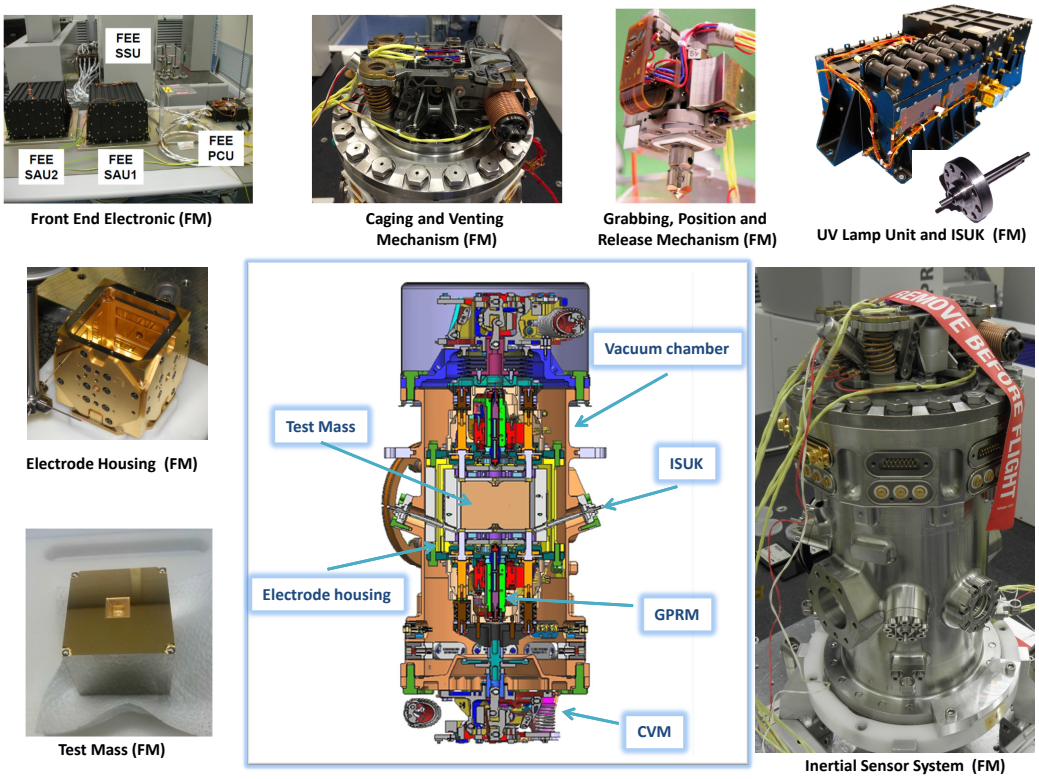

Figure 4. Schematic drawing and photographs of the Inertial Sensor Subsystem flight models (FM, courtesy of CGS). At the centre a section of the full model of the ISS. From bottom left: test mass and electrode housing (courtesy of CGS) ; GRS Front-End Electronics, Caging Mechanism (CM) composed by the Caging and Venting to space Mechanism (CVM) and the Grabbing Positioning and Release Mechanism (GPRM, courtesy of RUAG), UV Lamp Unit and a UV vacuum fibre feedthrough (Courtesy of ICL), Inertial Sensor Subsystem completely integrated (courtesy of CGS).

carefully also for their role in defining the performance of the test mass discharging system based on the UV photoelectric effect. It required extensive investigation of the overall process both through detailed simulation, experimental investigations on samples, and experiments performed in conditions as representative as possible of the hardware and of the operating conditions in flight, using the torsion pendulum facilities in Trento.

Finally, a challenging requirement arises in the need to reduce cross-talk and to reduce the GRS signal levels – and thus noise coming from sensing gain fluctuations – once the TM is aligned to the interferometry system, which requires geometrical tolerances in the range of 10-50 μm. Machining precision and clever design and assembly strategies have allowed this goal to be achieved without over-complicating the manufacturing process.

Following a demanding trade-off phase supported by an extensive and in-depth breadboarding activity, the industrial contractor, Compagnia Generale per lo Spazio (CGS), developed and qualified the two flight model electrode housings for LISA Pathfinder delivering them in October 2013. The electrode housing was realised as a molybdenum-sapphire composite structure where a molybdenum electrode cubic frame accommodates six faces with the electrodes made of gold-

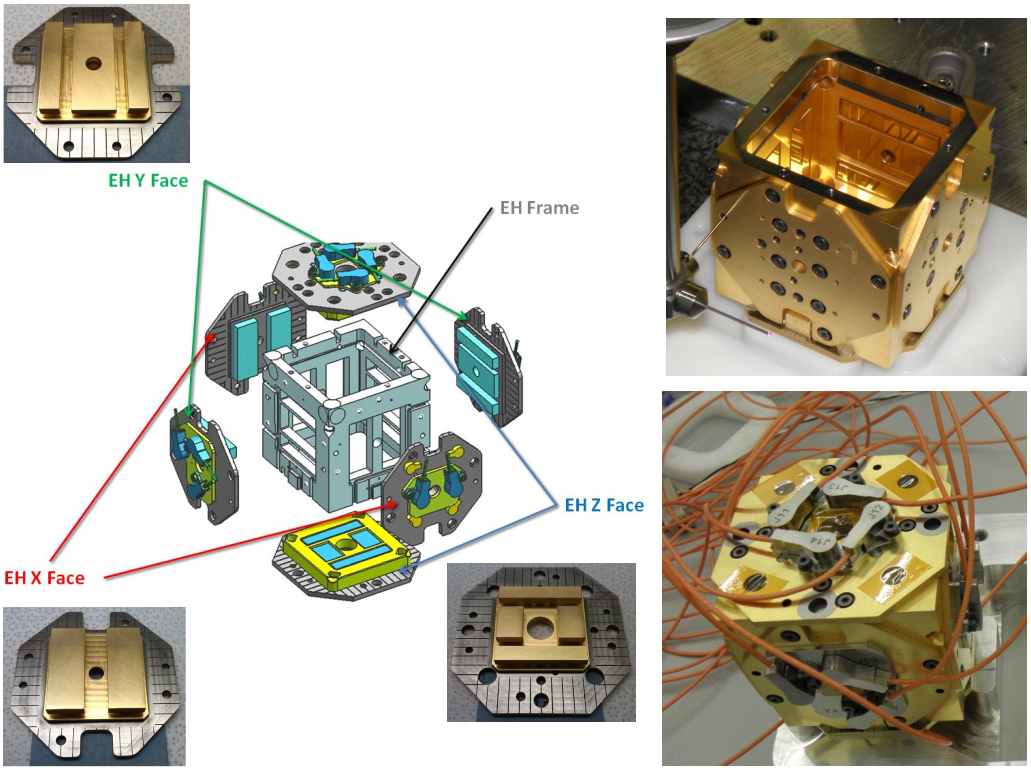

Figure 5. Flight Model electrode housing implementation: the exploded view shows the main parts of the electrode housing, including the electrode configurations on each face with their picture; on the top right, a photograph of the assembled electrode housing without one of the Z faces, showing how the electrode housing appears inside; bottom right, electrode housing completely assembled with connectors and cables (courtesy of CGS).

coated metal plates electrically isolated by means of sapphire spacers. All the inner surfaces facing the test mass are gold coated as well. An exploded view of this device is shown in Fig. 5, together with pictures of the flight model electrode housing at different integration stages and the inner side of the faces with the electrodes.

The GRS integration required analysis and design of gravitational compensation masses, with the final verification of the gravitational requirement based on a model calculated from measured values of the masses and positions of all the satellitеś elements. Before this final integration, a calibration test campaign was devoted to measure the sensitivity of the capacitive displacement sensor of the flight model electrode housing coupled to its front-end electronics (FEE) flight model. A white noise floor at the level of $\mathrm{aF}/\sqrt{\mathrm{Hz}}$ was also measured (Fig. 6), demonstrating the fulfilment of the required position sensitivity of $1.8\,\mathrm{nm}/\sqrt{\mathrm{Hz}}$.

Functional tests of the caging and vent mechanism (CVM), the TM launch lock device that provides a roughly 1200 N holding force, preventing damages due to vibrations at launch and opens the ISS vacuum chamber vent valve to space, and of the grabbing, positioning and release mechanism (GPRM), a second stage actuator that breaks the launch lock device adhesion to the TM and positions it before the final TM release phase, were carried out successfully.

The sensors are currently completing the final acceptance tests to pass to the next stage of

integration with the optical metrology: vibration and thermal vacuum tests on both ISS were successfully performed and now the final bakeout procedure and discharging management system test are ongoing.

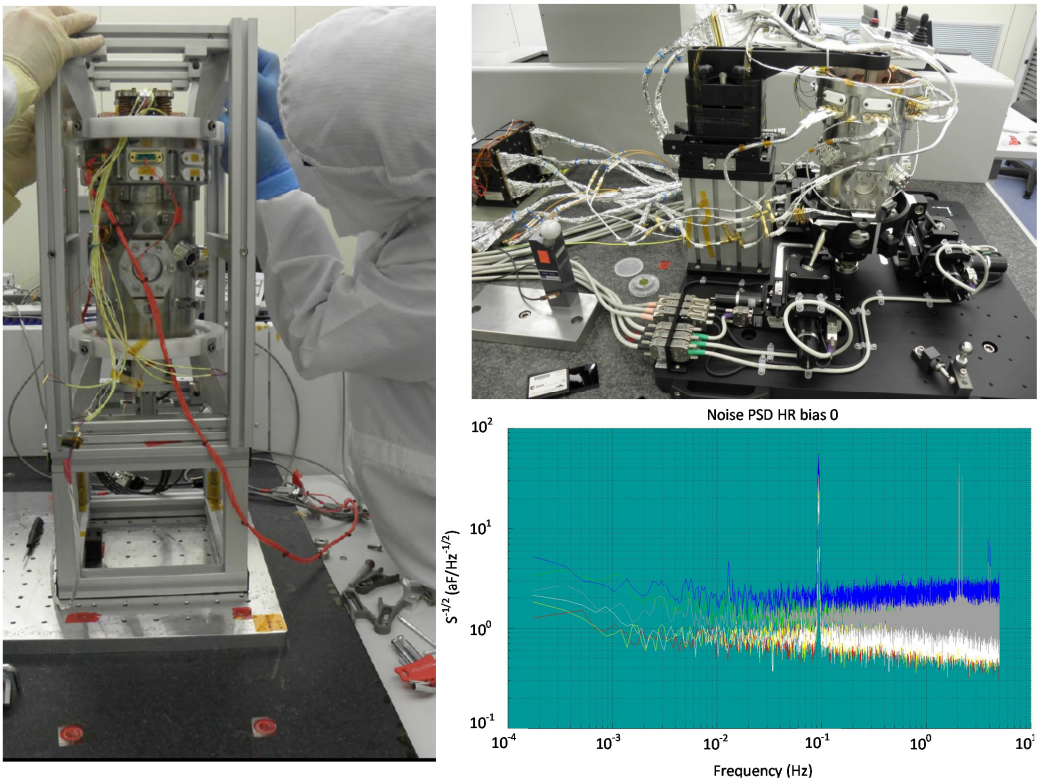

Figure 6. One of the Inertial Sensor Subsystems during the integration is shown in the picture on the left; the top right picture shows the calibration test set-up at the testing facility of Compagnia Generale per lo Spazio (CGS): it allowed the whole vacuum chamber, hosting the electrode housing connected to its flight model FEE to move in six degrees of freedom, with respect to the TM, while a CMM was used to verify the actual displacement within 1 μm accuracy ; bottom right, a plot of the white noise floor of the six capacitive readout channels of one of the ISS, that are at the level of aF/$\sqrt{\text{Hz}}$ in the measurement frequency bandwidth, in compliance with the required position sensitivity of 1.8 nm/$\sqrt{\text{Hz}}$ (courtesy of CGS).

3.2. The LISA Pathfinder Optical Metrology System

The aim of the Optical Metrology System (OMS) is to measure the relative displacement between the two TMs along the axis between them [15]. A secondary aim is to measure the two relative angular displacements of the test masses about this axis. The overall requirements are that the OMS should be able to measure the relative displacemets of the test masses with a noise level of below 6.5pm/$\sqrt{\text{Hz}}$ in the measurement band of $3 - 10$ mHz. The angular measurement is achieved by a technique known as differential wavefront sensing (DWS) and has a target sensitivity of 2×10^{-8}rad/$\sqrt{\text{Hz}}$. The OMS is a complicated system with a number of different subsystems interlinked by various feedback control systems. An outline of the system and its interlinks can be seen in Figure 7

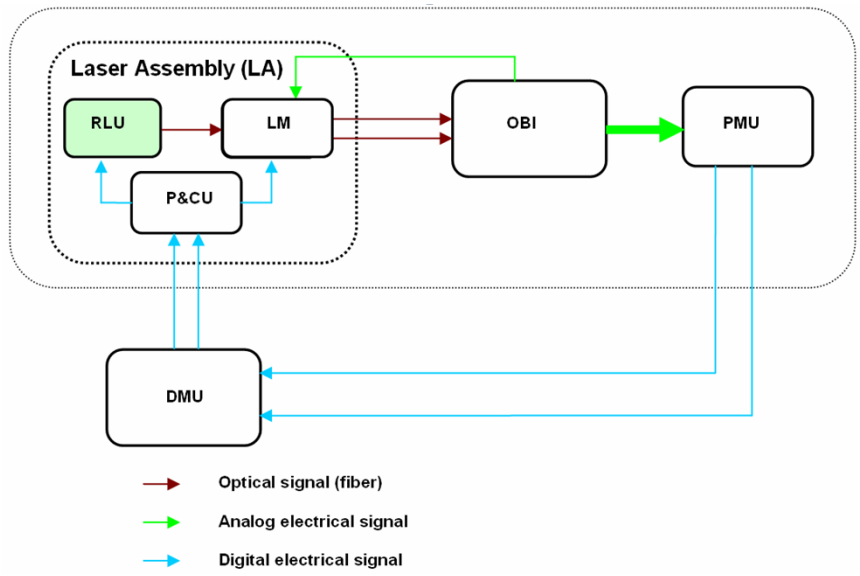

Figure 7. Diagram of the LPF OMS system showing the subsystems and their interlinks. The acronyms are explained in the text apart from the Power and Control Unit (P&CU).

- **Reference Laser Unit (RLU)** The RLU is the laser source for the OMS. The laser is an Nd:YAG NPRO operating at $\lambda = 1064\,\mathrm{nm}$, and producing 35 mW of single mode, single frequency light. The light is coupled into a polarisation preserving single mode optical fibre.
- **Laser Modulator (LM)** The LM takes light from the RLU fibre, splits it into two beams and frequency shifts each beam by slightly different frequencies, both around 80 MHz so that the resulting two beams have a controlled frequency separation of around 1kHz. These two beams are then coupled back into two optical fibres.
- **Optical Bench Interferometer (OBI)** The OBI takes light from the two feed fibres from the LM, collimates the output beams, and uses them to form 4 interferometers on the optical bench. The four interferometers are:
  - **Reference** interferometer that provides a reference phase signal that can also be used to stabilise the optical path onto the optical bench;
  - **x12** interferometer measures the relative displacement and angles between the two test masses, these are the main science signals;
  - **x1** interferometer measures the relative displacement and angles between test mass 1 and the optical bench;
  - **Frequency Noise** interferometer to measure laser frequency noise.

  To perform the measurement with the required accuracy the OBI must direct the beam onto the nominal test masses positions with an accuracy of $\pm 25\mu$m. The OBI must also be extremely stable and should add less than $1\mathrm{pm}/\sqrt{\mathrm{Hz}}$ of noise in the measurement bandwidth. The optical bench is constructed from Zerodur low expansion material with the critical components hydroxy-catalysis bonded to the Zerodur[16]. The layout of the OBI is shown in Figure 8.
- **Phasemeter Unit (PMU)** Each interferometer is read out by two quadrant photodiodes for redundancy. The PMU takes the electrical signals from all of the quadrant photodiodes.

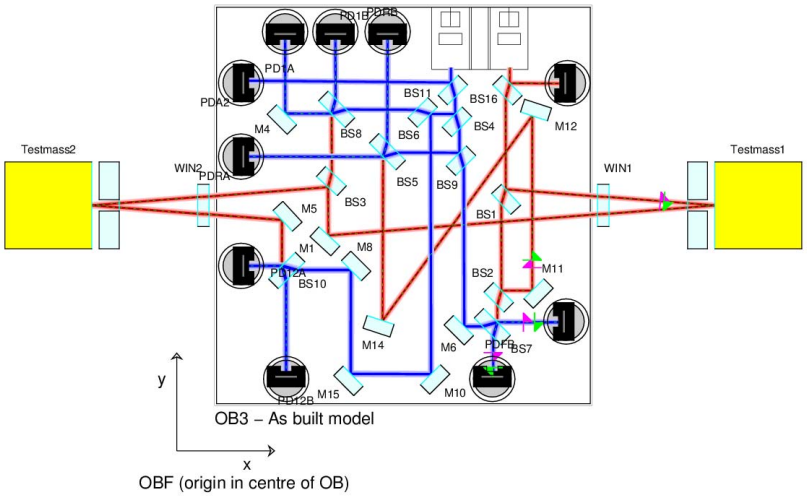

Figure 8. The optical model of the OBI. This is the as-built model. The two different laser frequencies are shown in different colours.

It calculates the phase of the heterodyne signal in each quadrant using a single bin discrete Fourier transform, and passes this data, plus the average light level to the DMU.

- **Data Management Unit (DMU)** The DMU is responsible for data handling for many of the LTP subsystems. One of its tasks is to take the signals from the PMU, process them to produce the required optical longitudinal and DWS signals. It also communicates relevant optical signals to other systems such as the Drag Free and Attitude Control System.

3.3. On station thermal test campaign

Throughout the Manufacture of the flight system, individual units were thoroughly tested, however it was only in October and November of 2011 that all of the subsystems were assembled together and their integrated performance tested as part of the On Station Thermal Test campaign (OSTT)[17]. All of the OMS systems used in the test were flight or flight-equivalent items, however the test masses were replaced by rigidly mounted dummy mirrors. The test were carried out in a vacuum and thermal environment representative of that endured by the spacecraft. The OMS performance met its requirements for both longitudinal and angular sensing. A graph of the longitudinal sensing performance is shown in Figure 9.

4. Operations and Data Analysis

The science operations phase of the LISA Pathfinder mission that focusses on the optimisation and characterisation of the LTP instrument, and the LPF satellite as a whole, takes place immediately after the industrial commissioning phase, and will last for around 90 days.

Each of these days will be packed with investigations and measurements with the aim of meeting the two primary scientific goals of the mission:

- Demonstrate the quietest possible test-mass free-fall by minimising the relative residual acceleration of the test-masses;

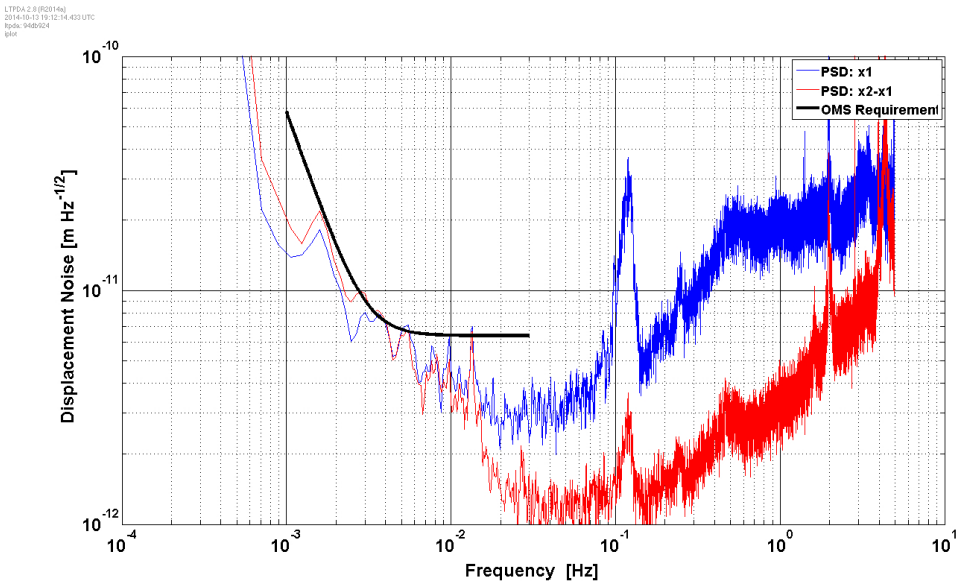

Figure 9. Longitudinal sensing noise of the OMS during the OSTT campaign. The noise is comfortably below requirement which is shown as the bold black line.

- Develop a detailed physical noise model of the entire system, showing the contribution of all the main disturbances to the obtained free-fall.

4.1. Science Investigations

Achieving these goals requires a careful planning and scheduling of the different experiments which can be carried out on-board the satellite. Table 1 lists examples of the experiments which will be performed at some stage of the operations phase, grouped into broad categories. The exact ordering of the investigations will, of course, depend somewhat on the results obtained, and as such can only be tentatively planned in advance. Nonetheless, due to the constraints on the mission planning, a consolidated time-line of investigations needs to be available two weeks in advance at all stages of the mission. As such, the initial weeks of the science operations phase have already been planned.

An example of such an investigation is the system identification investigation designed to probe the primary parameters which influence the two main Drag-Free and Attitude Control (DFACS) loops: the drag-free loop which maintains the SC centred on the reference test-mass, and the x-axis suspension loop which maintains the second test-mass at a fixed distance from the reference test-mass. This investigation involves injecting a sequence of sinusoidal signals into the set-points of the two loops. Figure 10 illustrates the first part of this investigation, the injection into the drag-free loop, and shows the signals from a simulation.

Planning and scheduling an investigation requires a number of activities to take place. Firstly, the investigation must be carefully designed to allow extraction of the desired physical measurements with the desired accuracy, and in the shortest amount of time possible. Following that, the design has to be rationalised to meet the constraints of the system, ensuring the correct commanding is used, and that the state of the instrument is appropriate. Next, the investigation must be simulated on the mission simulator, first in isolation to verify the commanding, and then, ideally, as part of a larger time-line, to help evaluate any constraints that may be present due to previous investigations, or that may be imposed on following investigations.

Residual Force Noise Measurements	
1	Noise performance baseline and tracking
2	Noise correlations with other measured quantities
3	Assessment of low-frequency (sub-milliHertz) performance via extended (multi-day) noise measurements
4	Coupling of beam power fluctuations to test-mass motion via radiation pressure.
5	Contribution of test-mass charging and stray potentials to the overall force noise budget.
System Identification	
5	The estimation of the primary parameter which affect the two x-axis DFACS loops. These have most impact on our ability to estimate the residual differential test-mass acceleration and include such quantities as the thruster and capacitive actuation gains, the "stiffness" couplings and the system delays.
6	Assessment of the main cross-talk effects which couple motion along/around other degrees-of-freedom into the primary science measurement. Investigations will be carried out to quantify the tilt-to-length coupling of the optical metrology system, sensing cross-talk of the GRS, actuation cross-talk in both the thrusters and the capacitive actuators, among others.
Optimisation of the Optical Metrology System	
7	Optimisation of the test-mass position along x to reduce the coupling of various noise terms into the main x-axis measurements.
8	Optimisation of the test-mass position along y and z to minimise the coupling of angular test-mass jitter into the x-axis measurements.
9	Optimisation of the various OMS-related control loops to minimise the noise contributions to the primary measurement.
Optimisation of the Gravitational Reference System	
10	Determine the best 3D operating point for each test-mass to minimise sensing noise.
11	Measurement and compensation of actuation cross-talk.
Characterisation of the thermal & magnetic environment	
12	Activation of heaters on electrode housings to estimate force effects excited due to thermal gradients.
13	Activation of heaters on the struts which support the optical bench, allowing characterisation of the effect of thermally driven distortions on the measured phase in the interferometers.
14	Probe phases distortions of the optical beams arising from thermal fluctuations of the optical windows which isolate the test mass enclosure from the optical bench environment by activating the heaters mounted on the optical windows.
15	Assess the contribution of fluctuating magnetic fields to the overall force noise budget by generating oscillating magnetic fields with the coils mounted outside the test-mass housings.

Table 1. Examples of some of the investigations that will be carried out on LPF during the science operations phase.

4.2. The Operational Environment

A tight, real-time interaction of the scientists and operations engineers is required if we are to extract the maximum science from the available operational days. This in itself places many requirements on the operational environment, including the development of dedicated planning tools which seamlessly allow a design conceived at the science planning stage to flow all the way through to a valid commanding file which can be passed on to the Mission Operations Centre for uploading to the satellite. A series of software tools have been developed to facilitate this process, and the entire end-to-end chain is currently being tested in a series of simulation runs.

Following the upload and execution of an investigation, the relevant data needs to be retrieved and delivered to the science teams for prompt analysis. This allows a relatively quick re-planning

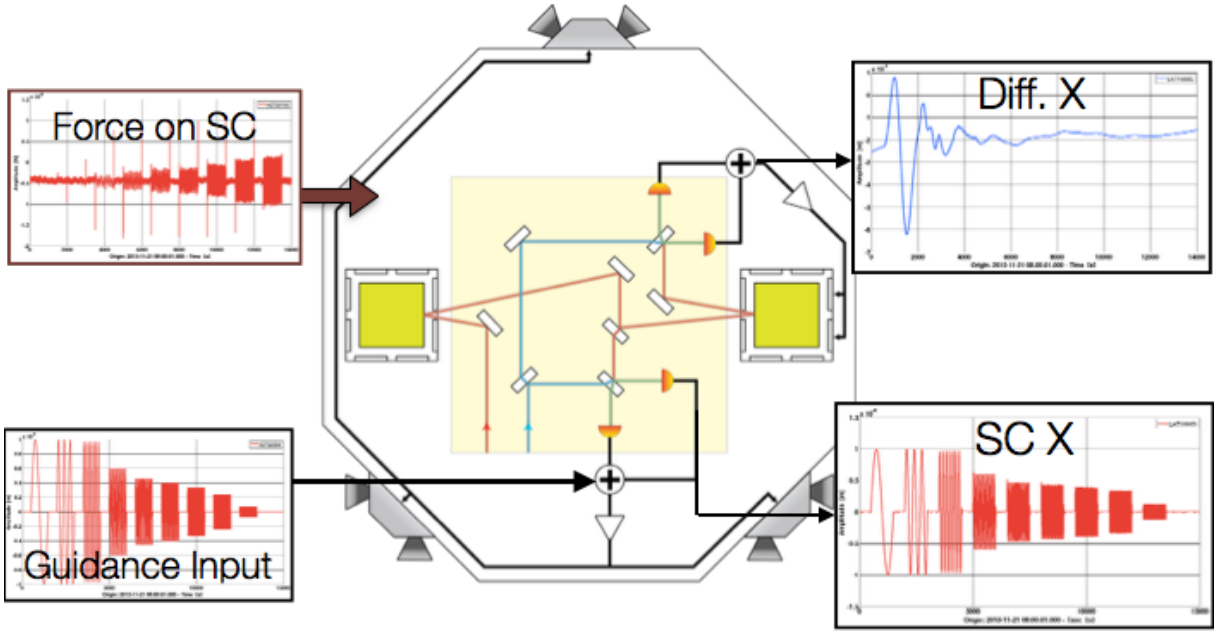

Figure 10. Schematic of LISA Pathfinder showing where, and what, signals are injected into the drag-free loop, and the expected output of the longitudinal interferometers.

cycle, giving the possibility of adapting the future mission time-line based on the results obtained to date.

The data analysis is carried out using a dedicated toolbox which is built on top of MATLAB. The LTPDA Toolbox provides an object-oriented data analysis environment with full history tracking of all processing steps which are performed on the data. The resulting analysis objects can be stored and retrieved from specially designed data repositories, giving the possibility for multiple analysis teams to access and share data concurrently. Figure 11 shows the flow of data through the various elements involved in analysing the data from LISA Pathfinder. In addition to the front-line analysis carried out at ESA's Science and Technology Operations Centre, off-line, in-depth analysis will be carried out at dedicated complementary data centres around Europe.

5. Conclusions

Throughout the history of the LISA/eLISA mission, the science return has never been in doubt - eLISA will observe the Universe in a way which has never been possible before. This has captured the imagination of the science community, but at the same time, mission studies have highlighted the challenging experimental metrology needed to realise such a revolutionary observatory. Together, these facts prompted the European Space Agency to adopt the LISA Pathfinder mission - the science return of a spaceborne gravitational wave detector easily justifies the technology development mission.

LISA Pathfinder is the first mission of its kind; the path from the original concept to the production of flight hardware has not been easy, however, it has been achieved. Production of the flight hardware is complete, with all units demonstrating that we can not only meet, but also exceed the performance requirements levied on the mission. The system is now entering the final tests, in preparation for the launch campaign.

LISA Pathfinder is scheduled to launch in mid-2015, with first performance results available

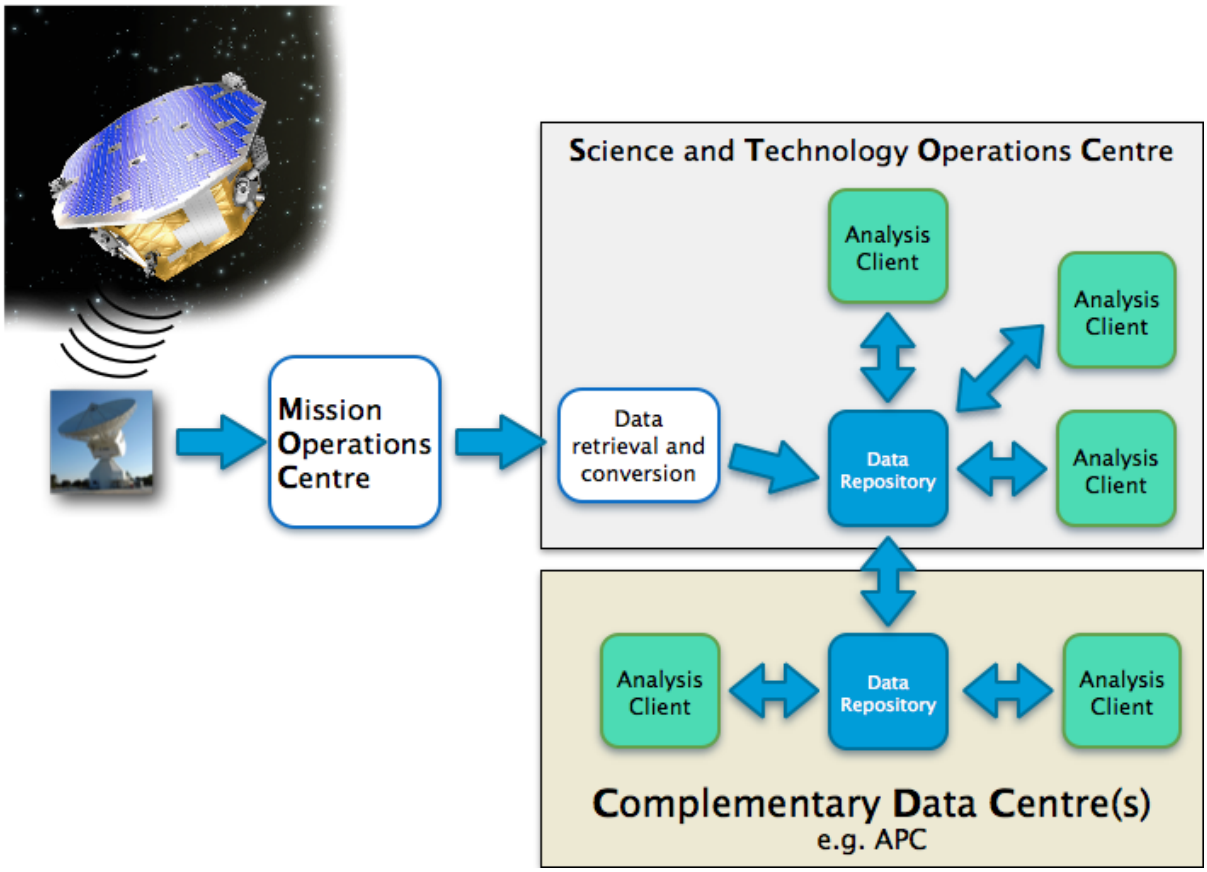

Figure 11. A schematic overview of the data downlink, showing the main elements of the science operations infrastructure and the route the telemetry takes through to the analysis by the on-duty scientists.

approximately three months thereafter.

Acknowledgments
The authors would like to thank the entire LISA Pathfinder team for their continued work in making the mission possible. The LISA Pathfinder mission is funded through the European Space Agency, while the LTP is funded by ESA, France, Germany, Italy, Netherlands, Spain, Switzerland, and the United Kingdom.

References

[1] Jennrich, O., *et al* , (2011) LISA - Unveiling a hidden Universe, *E*SA/SRE(2011)3 unpublished
[2] Jennrich, O., *et al* (2011) NGO - Revealing a hidden Universe: opening a new chapter of discovery, *E*SA/SRE(2011)19 unpublished
[3] Danzmann, K.D., *et al* (2013) The Gravitational Universe Whitepaper, available from *h*ttp://elisascience.org/whitepaper
[4] Committee for a Decadal Survey of Astronomy and Astrophysics (2010) New Worlds, New Horizons in Astronomy and Astrophysics, **ISBN: 0-309-15800-1**
[5] Danzmann, K.D., *et al* (1998) European LISA Technology: Demonstration Satellite for the LISA Mission in ESA's Space Science Programme, unpublished proposal
[6] Congedo G, *et al* 2013 *Phys. Rev. D* **88** 082003
[7] Vitale S 2014 *Gen. Relativ. Gravit.* **46** 1730
[8] Rummel R, Yi W, and Stummer C 2011 *J. Geodesy* **85** 777

[9] Bortoluzzi D, *et al* 2004 *Class. Quantum Grav.* **21** S573
[10] Antonucci F, *et al* 2011 *Class. Quantum Grav.* **28** 094002
[11] Grynagier A, Fichter W, and Vitale S 2009 *Class. Quantum Grav.* **26** 094007
[12] Canizares P, *et al* 2011 *Class. Quantum Grav.* **28** 094004
[13] Dolesi R *et al* 2003 *Class. Quantum Grav.* **20** 99
[14] Weber W J, *et al* , 2002 in Cruise, M., Saulson, P. (Eds.), *Proceedings of the SPIE Astronomical Telescopes and Instrumentation Conference* vol. 4856, SPIE Optical Engineering Press, Bellingham, WA, pp. 31?42
[15] Robertson D I, Fitzimmons E D, Killow C J, Perreur-Lloyd M, Bogenstahl J, Ward H 2007 Optical Bench Interferometer Detailed Design Document *Internal project document* **S2-UGL-DDD-3003)**
[16] Robertson D I, Fitzimmons E D, Killow C J, Perreur-Lloyd M, Bryant J, Cruise A M, Dixon G, Hoyland D, Smith D and Bogenstahl J, 2013 Construction and testing of the optical bench for LISA pathfinder *Classical and Quantum Gravity* **30(8)**
[17] Guzman Cervantes F, *et al.*, 2012 LISA Technology Package Flight Hardware Test Campaign *APS Conference Series* **467**
[18] Cruise A M, Hoyland D, and Aston S M 2005 Implementation of the phasemeter for LISA LTP *Classical and Quantum Gravity* **22** S165 - S169
[19] Heine, F, et al., Space qualified laser sources, Optical Sensing II - Proceedings of SPIE, 6189, 61892I (2006)